

F-1
NACA RM L57J14a



RESEARCH MEMORANDUM

TRANSONIC FLUTTER INVESTIGATION OF TWO 50° SEMISPAN
MODIFIED-DELTA WINGS WITH TIP AILERONS

By Robert J. Platt, Jr.

Langley Aeronautical Laboratory
Langley Field, Va.

CLASSIFICATION CHANGE

To UNCLASSIFIED

By Authority of TFR 55 dtd 10/5/61
Changed by *10* Date 2/12/90

CLASSIFIED DOCUMENT

This material contains information affecting the National Defense of the United States within the meaning of the espionage laws, Title 18, U.S.C., Secs. 793 and 794, the transmission or revelation of which in any manner to an unauthorized person is prohibited by law.

NATIONAL ADVISORY COMMITTEE FOR AERONAUTICS

WASHINGTON

February 17, 1958



NATIONAL ADVISORY COMMITTEE FOR AERONAUTICS

RESEARCH MEMORANDUM

TRANSONIC FLUTTER INVESTIGATION OF TWO 50° SEMISPAN
MODIFIED-DELTA WINGS WITH TIP AILERONS

By Robert J. Platt, Jr.

SUMMARY

Transonic flutter data have been obtained on two semispan modified-delta wings with tip ailerons. The models, which were swept back 50° at the leading edge, were mounted as cantilevers from the tunnel wall. The ratio of aileron rotational frequency to wing bending frequency was near a value of 1. The data were obtained in the Langley 8-foot transonic pressure tunnel over a Mach number range from 0.6 to 1.2.

In the low supersonic speed range the model with a plain tip aileron fluttered at dynamic pressures which were about 10 percent less than those in the subsonic speed range. Fewer flutter points were obtained on the model with a rear-cutout tip aileron, but, again, there was an indication of a decrease in the dynamic pressure for flutter as a Mach number of 1.0 was approached.

INTRODUCTION

Conventional ailerons are known to lose much of their control effectiveness at transonic and supersonic speeds. In recent years interest has been shown in the use of all-moving tip controls, especially for delta wings, as a substitute for the conventional aileron. In reference 1, an extensive experimental investigation of the low-speed flutter characteristics of a semispan delta wing with an all-moving tip aileron was reported. The effects of center-of-gravity position and frequency ratio (ratio of aileron rotation to wing bending) were included. The investigation of reference 1 did not, however, examine the effect of compressibility on the flutter speed of a wing with a tip aileron.

Presented in the present report are the results of a transonic flutter investigation of two wing-aileron models at frequency ratios near 1, which in the tests of reference 1 resulted in the lowest flutter

~~CONFIDENTIAL~~

UNCLASSIFIED

speeds. Such frequency ratios were used in the present tests in order that the models would flutter within the tunnel operating limits. The two wing-aileron models embodied plan forms being considered for use on a ground-to-air guided missile. The models tested were semispan modified-delta wings with tip ailerons and were mounted as cantilevers from the tunnel wall. The Mach number range extended from 0.6 to 1.2.

SYMBOLS

c	section chord of model, measured parallel to stream direction, ft
EI	bending stiffness, lb-in. ²
f	natural frequency, cps
f _f	flutter frequency, cps
GJ	torsional stiffness, lb-in. ²
g	structural damping coefficient
I _{cg}	mass moment of inertia about axis through center of gravity, slug-ft ²
I _α	mass moment of inertia about elastic axis, slug-ft ²
M	free-stream Mach number
q	free-stream dynamic pressure, lb/sq ft
t	section maximum thickness, ft
T _t	stagnation temperature, °R

Subscripts:

h	first bending mode (wing with aileron)
β	aileron-rotation mode

APPARATUS AND METHODS

Wind Tunnel

The present investigation was conducted in the Langley 8-foot transonic pressure tunnel which is a closed-circuit, variable-density tunnel equipped with a slotted throat. The test section is approximately 86 inches by 86 inches in cross section with longitudinal slots in the upper and lower walls. The tunnel Mach number is continuously controllable through the transonic speed range up to a maximum Mach number of 1.2. The total pressure in the tunnel may be varied from about 0.25 atmosphere to 1.6 atmospheres, depending on the Mach number. The air is dried to eliminate condensation in the test section.

Models

Sketches of the two wing-aileron models tested are shown in figure 1, which gives their principal dimensions. The aileron of model 1 is termed a plain tip aileron, and that of model 2, a rear-cutout tip aileron. The airfoil sections were symmetrical circular-arc sections; however, the aileron tip was cut back at an angle of 45° , which resulted in a blunt trailing edge along the cutback portion of the tip. The airfoil sections varied in thickness-chord ratio as indicated in figure 1.

The models were of built-up metal construction with a single steel I-beam wing spar and aluminum-alloy ribs. The model skin was 0.032-inch sheet aluminum alloy bonded to the structure.

Some details of the aileron hinge mechanism are shown in figure 1(a). The aileron rotated about a steel hinge tube fitted with one ball bearing and one needle bearing and was restrained by a steel spring, one end of which was fixed to the hinge tube. The spring, which simulated the aileron actuator stiffness, was of such design that the spring stiffness increased greatly for aileron deflections beyond approximately 2° . This nonlinearity was designed into the aileron spring in an attempt to limit the aileron deflection and the flutter to a relatively safe amplitude.

Photographs of model 1 mounted in the tunnel are shown in figure 2. The semispan models were mounted rigidly to a base which was bolted to the tunnel wall. The purpose of this base was to move the models out of the wall boundary layer. The models were set at an angle of attack of 0° .

Calculated physical characteristics of the two models, as provided by the contractor, are given in tables I and II and figures 3 and 4.

Tables I and II present the calculated mass distribution and moments of inertia associated with each spanwise station. Complete stiffness data were not available; however, figure 3 gives the bending stiffness, calculated on the assumption that bending is resisted only by the spar. Figure 4 gives the torsional stiffness, calculated on the assumption that torsion is resisted only by the skin.

The contractor also provided experimental values of the uncoupled resonant frequencies, damping, and node-line locations. These frequencies and damping values are given in table III for the two configurations for which flutter was obtained. The node-line locations are shown in figure 5.

Instrumentation and Tests

Strain gages were mounted on the wing spar and on the aileron spring to give an indication of the start of flutter and to provide a record of the oscillations from which the frequencies could be obtained. The strain-gage signals were fed to opposite axes of an oscilloscope for a visual indication of flutter during the run and were recorded by a magnetic tape recorder. Two 16-millimeter motion-picture cameras (200 to 250 frames per second) were used to photograph the motion of the models.

The procedure used in making the tests was to evacuate partially the tunnel, raise the tunnel speed to the desired Mach number, and slowly increase the tunnel stagnation pressure until the model fluttered. As the pressure was increased, a continuous record of the strain-gage signals was made with the magnetic tape recorder. When the model fluttered, the tunnel total pressure and Mach number were recorded and motion pictures were taken, after which the pressure and speed were quickly decreased to prevent destruction of the model. In most cases the tunnel was stopped after each flutter point and the model was inspected for damage. After the run, the tape recording was played back and a visual record was obtained, by means of a recording oscillograph, of the strain-gage signals at flutter.

As the tests progressed, several checks were made on the uncoupled wing bending and aileron rotational frequencies, and on the damping. The wing bending frequency, measured with the aileron in place and restrained in rotation by small clamps at the leading and trailing edges, was found to be affected by the tension on the mounting bolts, which passed through the tunnel wall. When a change in the bending frequency was found, the mounting bolts were adjusted to return the frequency to its original value before making the next run. In an effort to obtain an uncoupled aileron-rotation mode in the tunnel, the wing

was restrained with 2- by 4-inch wooden supports and shot bags laid on the wing, and the aileron was restrained in bending by a hinge-line clamp which was fitted with a bearing to permit aileron rotation. The amount of restraint that was obtained in the wind tunnel for this mode was not completely satisfactory and the tunnel shake-test information for the aileron-rotation mode is believed to be less accurate than that presented in table III, which was obtained by the contractor with the use of more massive fixtures.

RESULTS AND DISCUSSION

The flutter-speed data obtained are listed in table IV along with the frequencies and damping factors measured on the models in the tunnel before and after the runs. Flutter of these models was preceded by a region of low damping, characterized by a buildup and decay of oscillations of identical frequency for the wing and aileron. During flutter, the oscillations maintained a nearly constant amplitude. A portion of an oscillogram illustrating the beginning of flutter is shown in figure 6.

As table IV indicates, the flutter frequency was very near the wing bending and aileron rotational frequencies. All the flutter points obtained on these two models appeared to involve wing bending and aileron rotation.

The flutter encountered was sometimes mild and the amplitude may have been limited by the built-in nonlinearity of the aileron spring. In the case of model 1, the flutter was mild at all Mach numbers except at $M = 1.212$ during run 3 when model 1 was damaged and had to be removed from the tunnel for extensive repairs. In the case of model 2, the flutter was mild only at $M = 0.798$ (run 7) and was rather violent at both higher and lower Mach numbers.

The flutter-speed data for model 1 (plain tip aileron) are plotted in figure 7(a) as the variation with Mach number of the dynamic pressure required to initiate flutter. The figure indicates that the dynamic pressure was nearly constant up to a Mach number of 0.9, decreased about 10 percent in the interval between $M = 0.9$ and 1.0, and remained nearly constant thereafter.

Some difficulty was experienced in reaching flutter with model 2 (rear-cutout aileron) within the operating limits of the wind tunnel. As table IV indicates, flutter was not obtained in the first run made with model 2 (run 4). Although not shown in table III, the aileron rotational frequency, with the aileron spring used for run 4, was 49.9 cycles per second, as measured by the contractor. A stiffer aileron actuator spring was then substituted and the tension on the tunnel-wall mounting bolts was decreased. These changes increased f_{β}/f_h from a

value slightly less than 1 to a value slightly greater than 1 and four flutter points were then obtained with model 2 before severe damage to the model occurred. These flutter data are plotted in figure 7(b). Few data points were obtained, but as with model 1, there is an indication of a decrease in dynamic pressure required to start flutter as $M = 1.0$ is approached.

The flutter characteristics shown in figure 7 are for models with ratios of aileron rotational frequency to wing bending frequency near 1. At other frequency ratios the variation of dynamic pressure at flutter with Mach number might be very different.

CONCLUDING REMARKS

Transonic flutter data have been obtained on two semispan modified-delta wings with tip ailerons. The Mach number range extended from 0.6 to 1.2. The ratio of aileron rotational frequency to wing bending frequency was near a value of 1.

In the low supersonic speed range the model with a plain tip aileron fluttered at dynamic pressures which were about 10 percent less than those in the subsonic speed range. Fewer flutter points were obtained on the model with a rear-cutout tip aileron, but, again, there was an indication of a decrease in the dynamic pressure for flutter as a Mach number of 1.0 was approached. The variation of dynamic pressure at flutter with Mach number might, however, be very different at other ratios of aileron rotational frequency to wing bending frequency.

Langley Aeronautical Laboratory,
National Advisory Committee for Aeronautics,
Langley Field, Va., September 30, 1957.

REFERENCE

1. Gaukroger, D. R.: Wind-Tunnel Flutter Tests on a Delta Wing With an All-Moving Tip Control Surface. R. & M. No. 2978, British A.R.C., Oct. 1953.

TABLE 1.- CALCULATED MASS DISTRIBUTION AND MOMENTS
OF INERTIA FOR MODEL 1

Spanwise station, in.	Mass, slugs	Distance from center of gravity		I_{cg} , slug-ft ² , about -		I_{α} , slug-ft ²
		Wing root, in.	Wing trailing edge, in.	Y-axis	X-axis	
0	0.0642	0	23.45	0.0622		0.0723
3.748	.1472	3.748	23.45	.1427		.1657
7.496	.1294	7.496	21.28	.0808		.0867
11.244	.0773	11.244	20.33	.0392		.0406
14.992	.0977	14.992	19.69	.0470		.0477
18.74	.0360	18.74	18.22	.0189		.0189
Wing	.5518	8.211	21.497	.4020	0.1124	.4319
18.74	.0597	18.74	17.72	.0115		.0120
24.39	.0553	24.39	17.12	.0115		.0125
30.04	.0190	30.04	15.44	.0033		.0042
35.70	.0031	35.70	15.10	.0003		.0005
Aileron	.1371	22.97	17.10	.0274	0.0137	.0292

TABLE II.- CALCULATED MASS DISTRIBUTION AND MOMENTS
OF INERTIA FOR MODEL 2

Spanwise station, in.	Mass, slugs	Distance from center of gravity		I_{cg} , slug-ft ² , about -		I_{α} , slug-ft ²
		Wing root, in.	Wing trailing edge, in.	Y-axis	X-axis	
0	0.0770	0	23.28	0.0722		0.0834
4.216	.1416	4.216	23.05	.1276		.1462
8.432	.1311	8.432	21.28	.0818		.0879
12.648	.1117	12.648	20.08	.0495		.0510
16.864	.0457	16.864	15.65	.0151		.0180
21.080	.0123	21.080	11.57	.0028		.0071
Wing	.5194	7.981	21.076	.3734	0.1032	.3936
18.739	.0615	18.739	21.26	.0075		.0103
22.978	.0640	22.978	16.47	.0232		.0254
27.217	.0138	27.217	14.71	.0022		.0038
31.456	.0108	31.456	14.26	.0010		.0025
35.696	.0019	35.696	13.93	.0001		.0004
Aileron	.1520	22.406	18.05	.0419	0.0172	.0424

TABLE III.- UNCOUPLED MODES

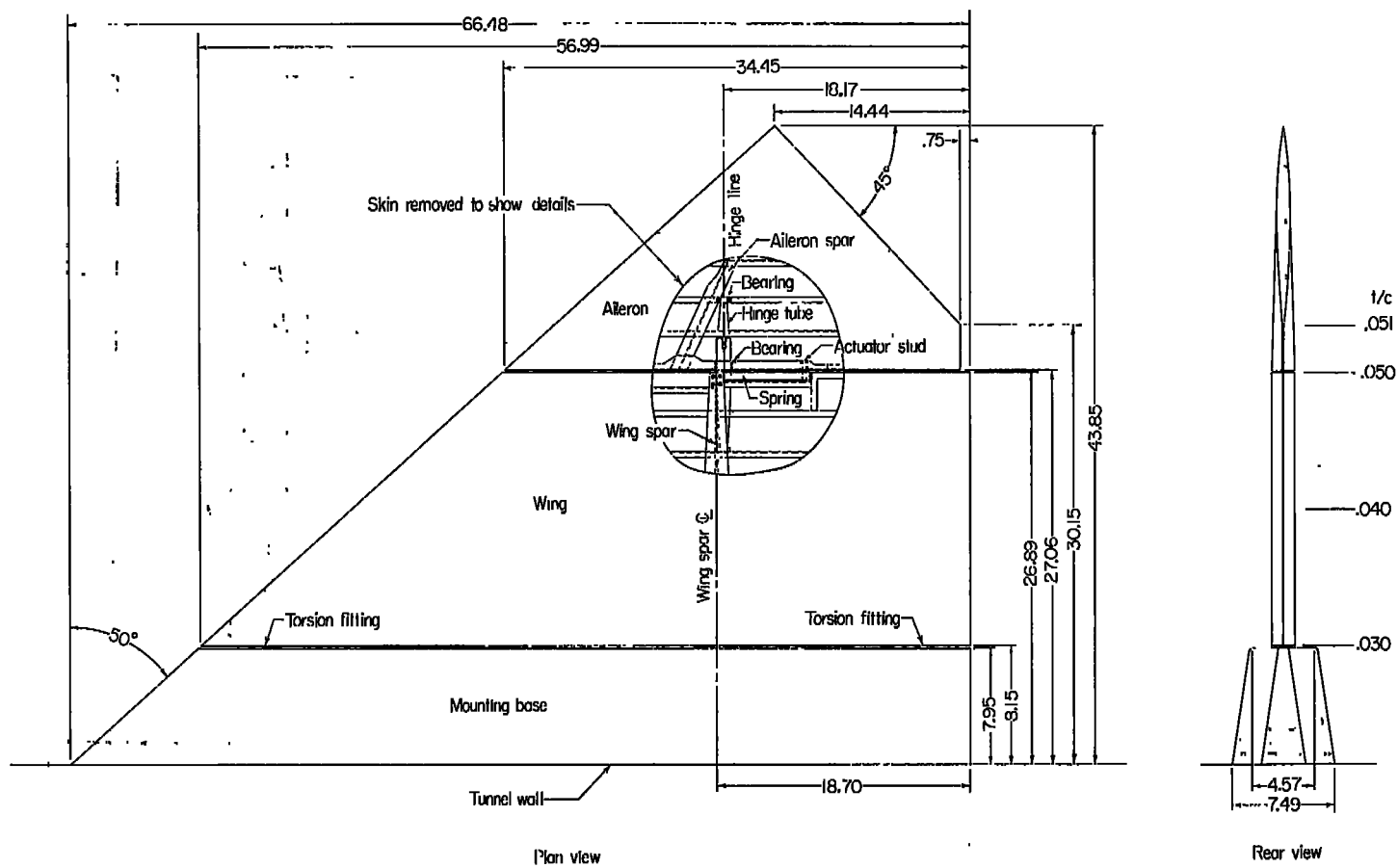
Mode	Model 1		Model 2	
	f, cps	g	f, cps	g
Wing bending	48.8	0.042	51.6	0.016
Aileron rotation	52.0	.070	54.7	.091
Aileron bending	91.1	.154	88.7	.238
Wing torsion	96.3	.009	91.0	.009

TABLE IV.- EXPERIMENTAL FLUTTER DATA

Run (a)	Model	M	$T_t,$ $^{\circ}R$	$q,$ lb/sq ft	$f_f,$ cps	Before run					After run					
						$f_h,$ cps	$f_{\beta},$ cps	f_{β}/f_h	ξ_h	ξ_{β}	$f_h,$ cps	$f_{\beta},$ cps	f_{β}/f_h	ξ_h	ξ_{β}	
1	1	1.112	584	463	51.8	49.2	51.5	1.05	0.020	0.127	49.3			0.029		
2	1	.599	584	508	51.8	49.3					50.7					
		.895	584	513	50.7											
3	1	1.212	584	454	49.6	49.3			.019							
4	2	^b 1.000	^b 584	^b 818	----	51.8	50.0	.97			.166	51.1			.022	
		^b .795	^b 584	^b 976	----											
5	2	1.000	574	383	48.4	47.6	56.8	1.19	.018							
6	2	.597	579	446	47.2	47.3			.016		45.4					
7	2	.798	575	486	48.0	47.8	52.1	1.09	.023	.120	47.8	52.5	1.10	.018	0.087	
8	2	.999	584	406	47.6	47.9	52.8	1.10	.025	.097	47.8			.017		
9	1	.999	563	451	52.2	49.2	52.9	1.08	.023	.085	49.0	52.5	1.07	.024	.125	
10	1	.900	580	492	51.5	49.1	53.6	1.09	.022	.075	49.2	53.6	1.09	.022	.126	

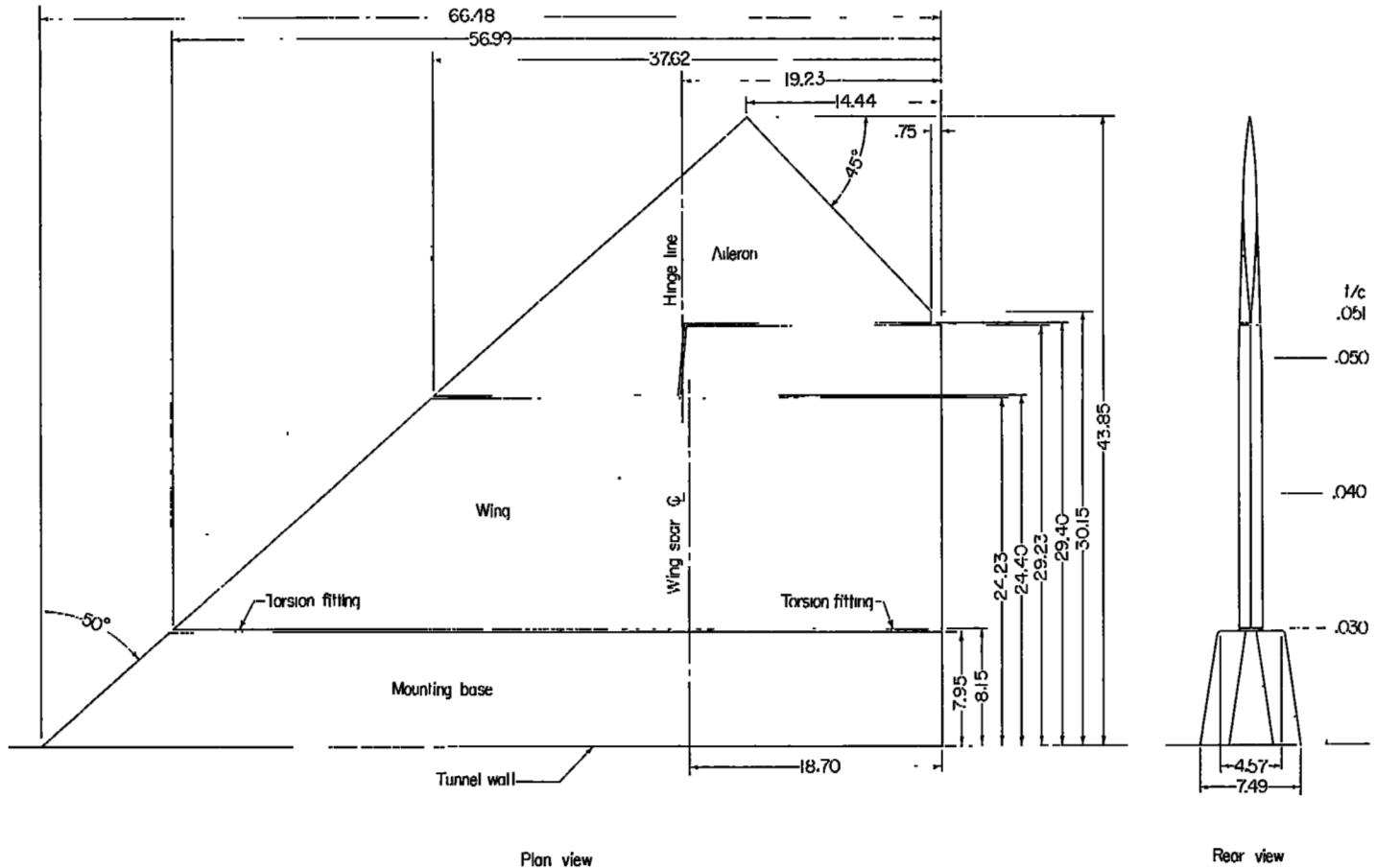
^aA run begins when the tunnel fan is started and ends when the fan is stopped.

^bFlutter was not encountered at this Mach number up to the value of dynamic pressure shown.



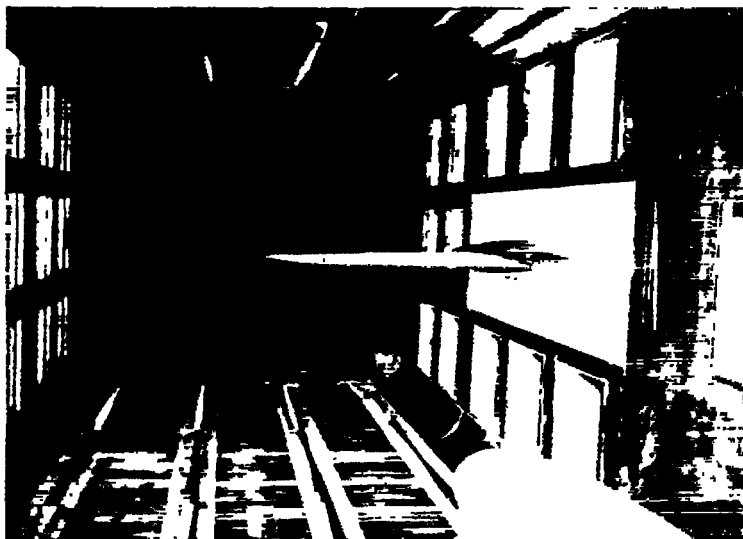
(a) Model 1 (wing with plain tip aileron).

Figure 1.- Models tested in the Langley 8-foot transonic pressure tunnel. All dimensions are in inches.



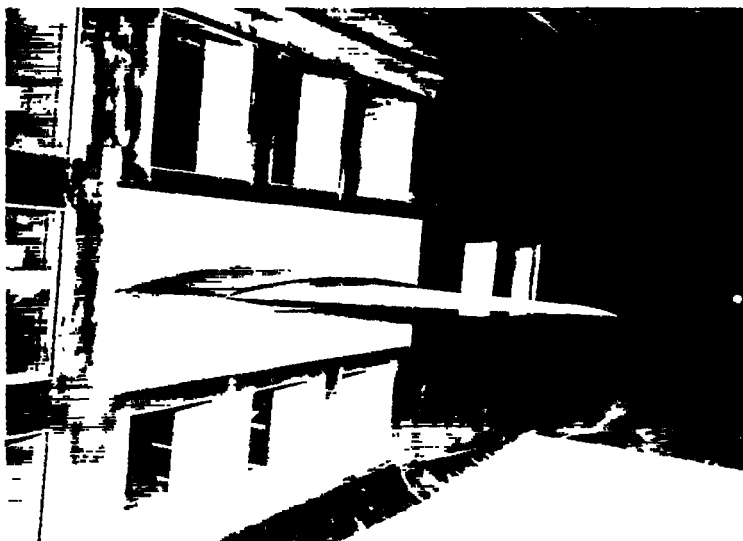
(b) Model 2 (wing with rear-cutout tip aileron).

Figure 1.- Concluded.



(a) Rear view.

L-94987



(b) Front view.

L-94988

Figure 2.- Model 1 in the Langley 8-foot transonic pressure tunnel.

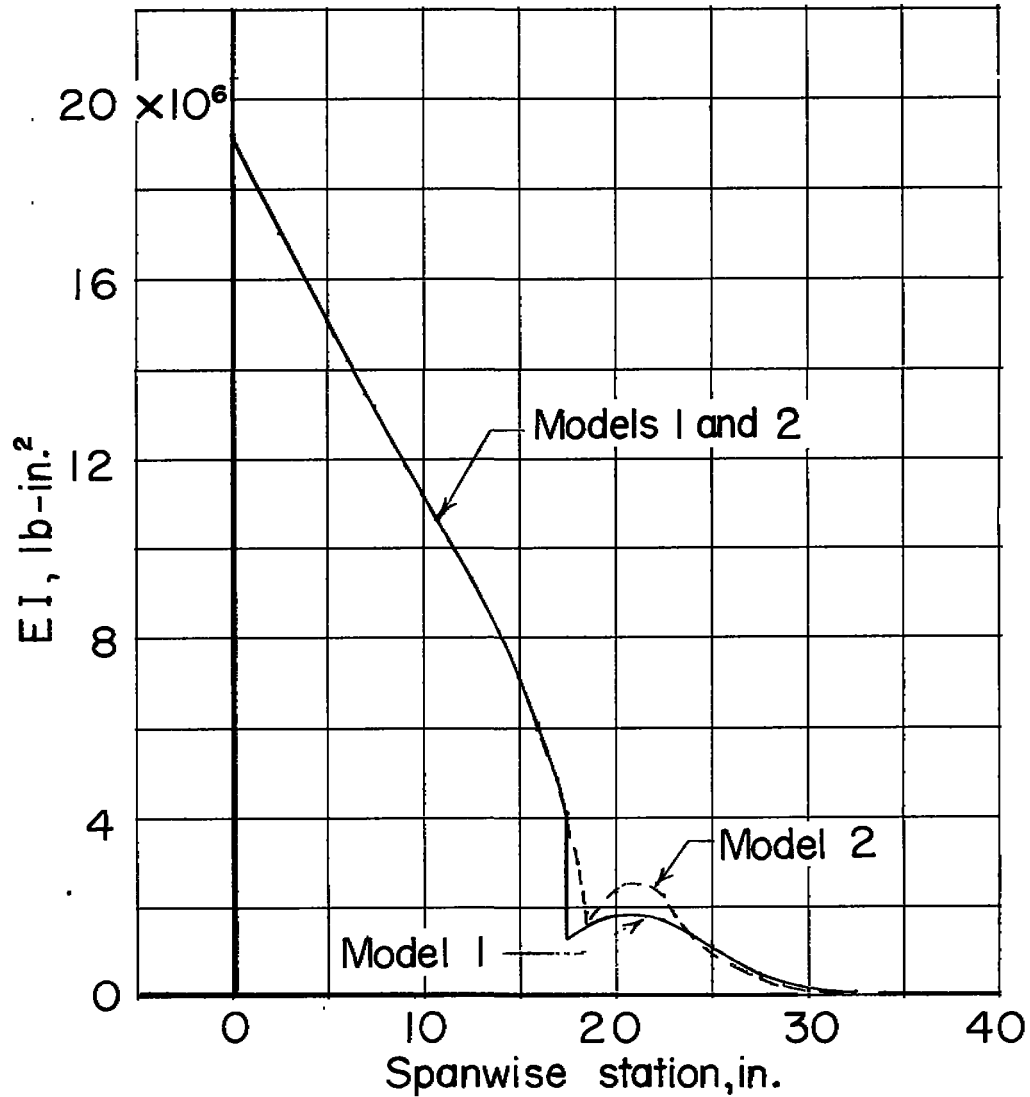


Figure 3.- Calculated bending stiffness of wing aileron, based on assumption that bending is resisted only by the spar.

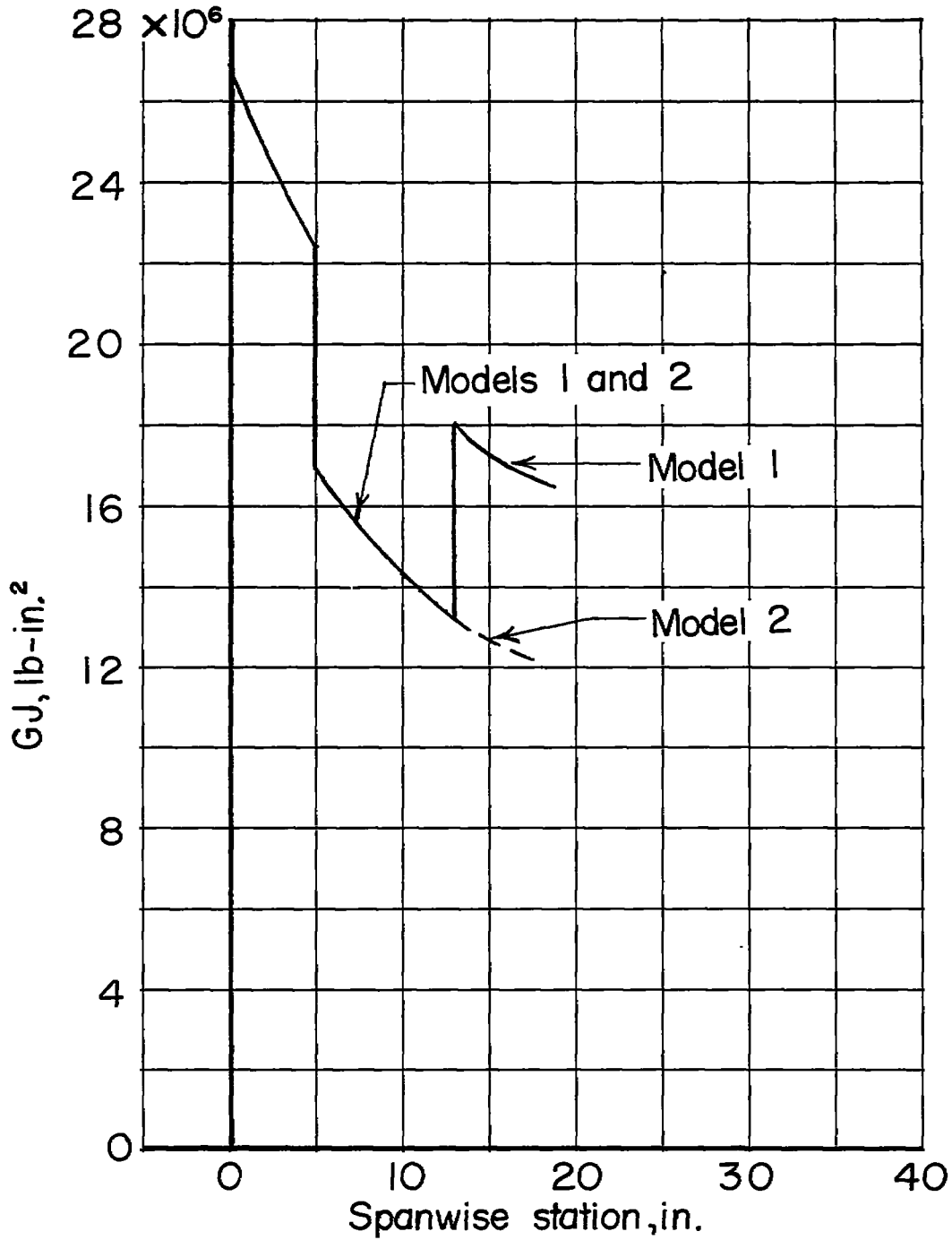
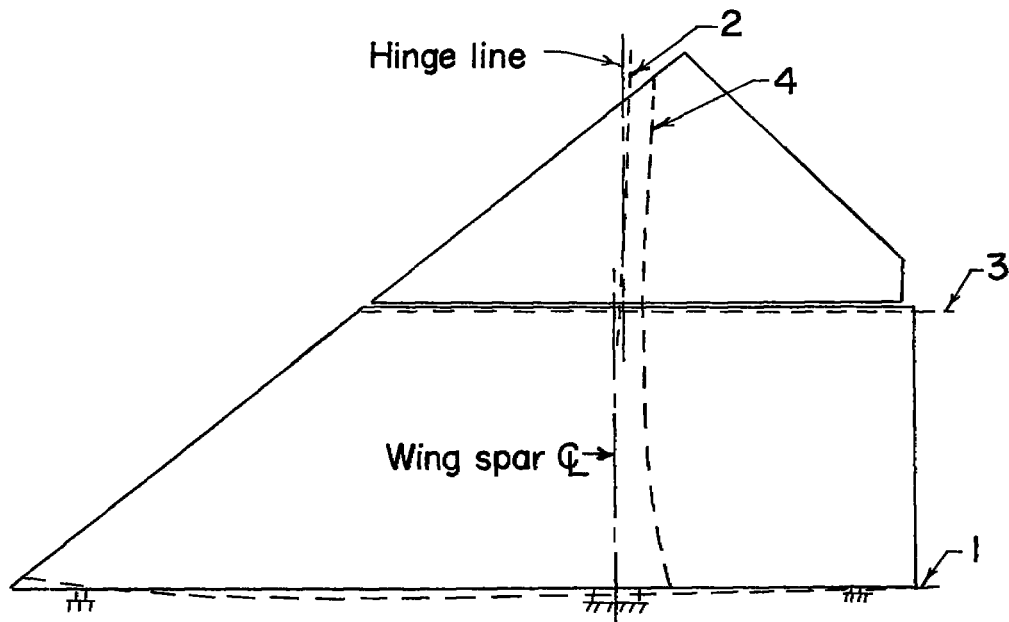
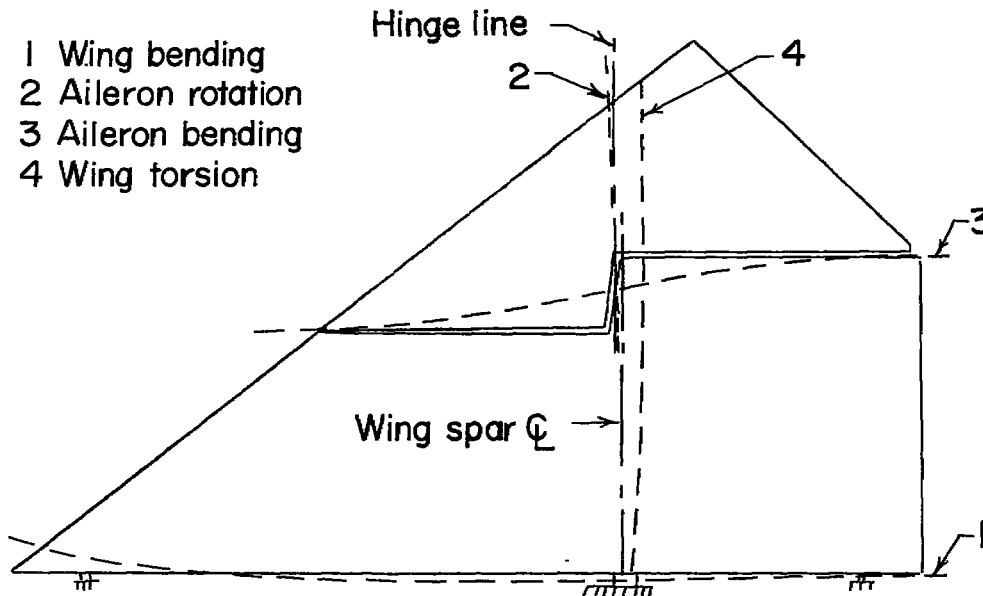


Figure 4.- Calculated torsional stiffness of wing, based on assumption that torsion is resisted only by the skin.



(a) Model 1 .



(b) Model 2 .

Figure 5.- Node-line locations for uncoupled resonant modes.

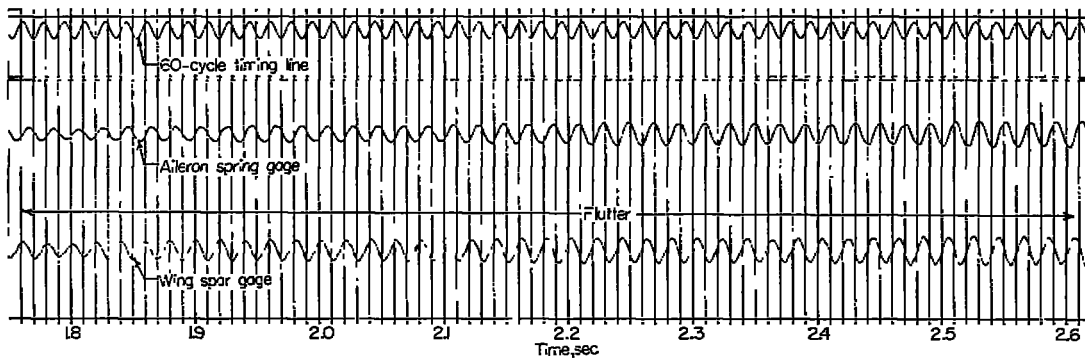
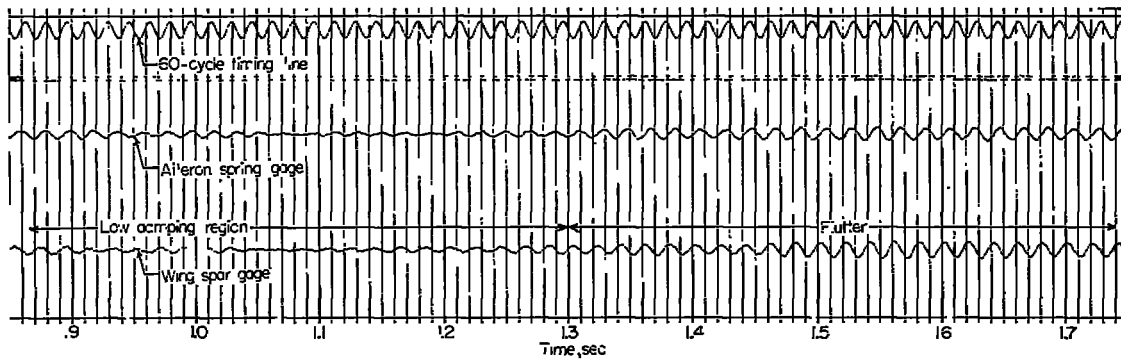
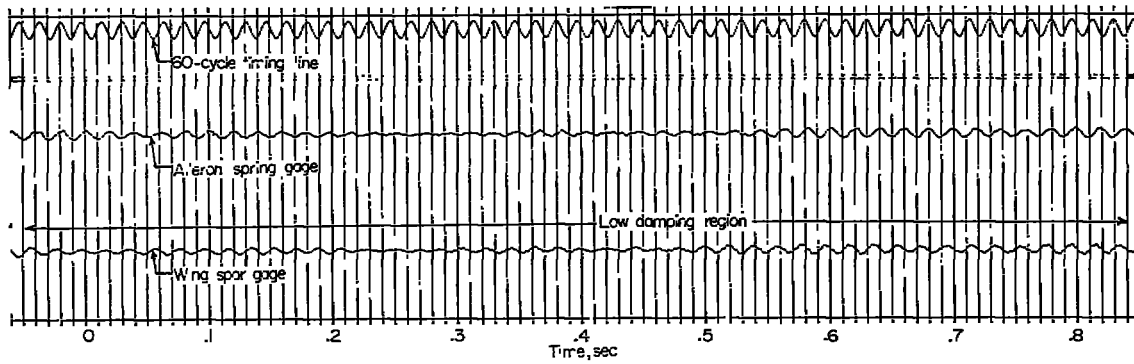


Figure 6.- Portion of oscillogram showing the beginning of flutter.
Model 1; run 3; $M = 1.212$.

UNCLASSIFIED

~~CONFIDENTIAL~~

NACA RM L57J14a

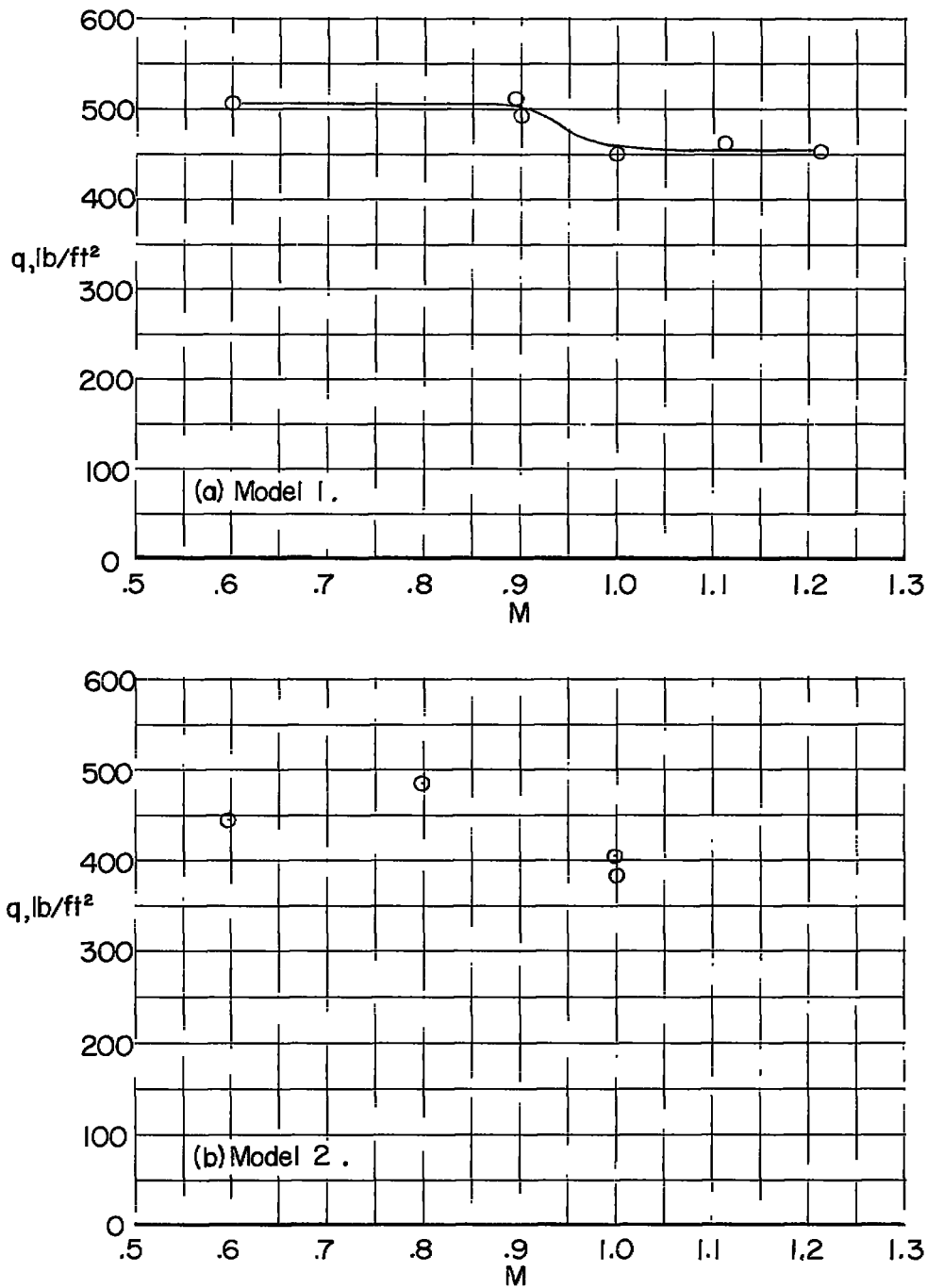


Figure 7.- Variation of dynamic pressure with Mach number for the beginning of flutter of the models.

UNCLASSIFIED

NACA - Langley Field, Va.

3 1176 01437 2578

UNCLASSIFIED

UNCLASSIFIED

